$^1J_{CP}$ = 17 Hz), 11.8 (dd, PMe_D, $^1J_{CP}$ = 31 Hz, $^3J_{CP}$ = 4 Hz), 22.8 (dd, PC_AH_2, $^1J_{CP}$ = 26 Hz, $^2J_{CP}$ = 11 Hz), 30.2 (dd, PC_BH_2, $^1J_{CP}$ = 31 Hz, $^2J_{CP}$ = 23 Hz), 33.2 and 35.9 (s, diastereotopic CMe_2), 38.6 (d, CMe_2, $^4J_{CP}$ = 3 Hz), 52.2 (s, Me_2CCH_2), 66.8 (d, OCH_2, $^3J_{CP}$ = 8 Hz), 122.7, 122.8 (s, CH aromatics), 124.1 and 135.5 (d, CH aromatics, J_{CP} = 6 and 10 Hz respectively), 153.8 (d, quaternary aromatic, J_{CP} = 5 Hz), 166.2 (dd, aromatic C bound to Ni, $^2J_{CP}$ = 88 Hz, $^2J_{CP'}$ = 32 Hz). Anal. Calcd for $C_{17}H_{30}OP_2Ni$: C, 55.0; H, 8.1. Found: C, 53.0; H, 8.1.

X-ray Structure Determinations. A summary of the fundamental crystal data for the compounds **1** and **2** is given in Table I.

Compound 1. A yellow crystal of irregular shape was epoxy resin coated and mounted in a Kappa diffractometer. The cell dimensions were refined by least-squares fitting the values of 25 reflections with $1 < \sigma < 22$ and the (h,k,l) range from (−8, 0,0) to (8,19,12) was measured with Mo Kα radiation (λ = 0.71069 Å) and $\omega/2\theta$ scan technique. The crystal became damaged by radiation. The intensities were scaled from the variation of three standard reflections whose intensities fell to 40% at the end of the data collection. The intensities were corrected for Lorentz and polarization effects and 1439 of these were considered as observed with $I > 3\sigma(I)$. Scattering factors for neutral atoms and anomalous dispersion corrections for Ni and P were taken from a standard reference.[50] The structure was solved by Patterson and Fourier methods. Anisotropic full-matrix least-squares refinement with unit weights, minimizing $\sum\omega(|F_o| - |F_c|)^2$ lead to R = 0.083. Final refinement with fixed isotropic temperature factors and coordinates for H atoms gave R = 0.077 and R_w = 0.090. No trend in ΔF vs F_o or sin θ/λ was observed. Most of the calculations were carried out with the X-RAY 80 system.[51]

(50) *International Tables for X-ray Crystallography*; Kynoch Press: Birmingham, U.K., 1974; Vol. IV, pp 72–98.

(51) Stewart, J. M. *The XRAY 80 System*; Computer Science Center, University of Maryland: College Park, MD, 1985.

Compound 2. A yellow prismatic crystal (0.5 × 0.3 × 0.2 mm) was sealed under nitrogen in a glass capillary, and data were collected on a Enraf-Nonius CAD4-F diffractometer. The structure was solved by heavy-atom methods; 3267 independent reflections were measured, of which 2020 were considered observed after the criterion $I > 3\sigma(I)$, and used in the refinement with anisotropic parameters for all non-hydrogen atoms except the methyl carbons attached to phosphorus (2). Unit weights were used (no trend in ΔF vs F_o or sin θ/λ was observed), and at convergence, R_F = 0.067. An absorption correction was applied.[52]

Acknowledgment. Generous support of this work by the Agencia Nacional de Evaluación y Prospectiva is very gratefully acknowledged. M.P. thanks the Ministerio de Educación y Ciencia for support of a research grant.

Registry No. 1, 104090-29-1; **2**, 104090-31-5; **3**, 104090-32-6; **4**, 118977-58-5; **5**, 104090-30-4; **6**, 118921-59-8; **7**, 104090-26-8; **8**, 104090-27-9; **9**, 104090-28-0; $NiCl_2(PMe_3)_2$, 19232-05-4; Mg(CH_2CMe_2Ph)Cl, 35293-35-7; CO, 630-08-0; $\overline{CH_2CMe_2\text{-}o\text{-}C_6H_4C{=}O}$, 26465-81-6; PhC≡CPh, 501-65-5; CO_2, 124-38-9; CH_2O, 50-00-0; CS_2, 75-15-0; *trans*-Ni($COCH_2SiMe_3$)Cl(PMe_3)$_2$, 75982-73-9; *trans*-Ni(CH_2SiMe_3)Cl(PMe_3)$_2$, 75982-54-6; $O{=}\overline{CCH_2CMe_2\text{-}o\text{-}C_6H_4C(S)S}$, 118921-60-1.

Supplementary Material Available: Tables of final fractional coordinates and thermal parameters for **1** and **2** (4 pages); observed and calculated structure factors (38 pages). Ordering information is given on any current masthead page.

(52) Walker, N.; Stuart, D. *Acta Crystallogr., Sect. A* **1983**, *A39*, 158.

Chemical Oscillators in Group VIA: The Cu(II)-Catalyzed Reaction between Thiosulfate and Peroxodisulfate Ions[1]

Miklós Orbán[†] and Irving R. Epstein*[,‡]

Contribution from the Institute of Inorganic and Analytical Chemistry, L. Eötvös University, H-1443, Budapest, Hungary, and the Department of Chemistry, Brandeis University, Waltham, Massachusetts 02254. *Received August 1, 1988*

Abstract: Sustained oscillations in redox potential, pH, and the concentration of dissolved O_2 are reported in the Cu(II)-catalyzed reaction between $K_2S_2O_8$ and $Na_2S_2O_3$ in a stirred tank reactor. A range of steady states is found, most of which can be unambiguously designated as either high or low pH, but there is no evidence of bistability. A free-radical mechanism in which Cu(I), Cu(III), and the radicals $SO_4^{\bullet-}$ and $S_2O_3^{\bullet-}$ play key roles appears to be capable of accounting both for the observed kinetics (first order in $S_2O_8^{2-}$ and Cu(II), zeroth order in $S_2O_3^{2-}$) of the batch reaction and for the oscillations in the flow system.

The past decade has witnessed a virtual explosion in the number of reactions that exhibit chemical oscillation. The first successes in the search for new chemical oscillators were confined to reactions in which oxyhalogen species played the key roles.[2] Because they allow facile redox transformations among a large number of oxidation states, the group VIIA elements are excellent candidates for generating the autocatalytic buildup or decay of transient species that has proved to be conducive to oscillation and other forms of exotic dynamical behavior.

Like the halogens, the elements of groups VA and VIA possess many stable oxidation states and easily undergo redox reactions among these states. To date, no oscillatory reactions based on nitrogen or phosphorus chemistry have been reported. However, several chemical oscillators have been found in which oxygen and/or sulfur species provide the driving force. These include the sulfide–sulfite–oxygen–methylene blue,[3] hydrogen peroxide–sulfide,[4] Cu(II)-catalyzed hydrogen peroxide–thiosulfate[5] and hydrogen peroxide–thiocyanate,[6] and the Ag(I)-catalyzed sulfide–peroxodisulfate[7] reactions. Although none of these systems has been characterized in anything like the mechanistic detail available for several of the halogen-based oscillators, it is already clear that the group VIA oscillators show a far greater range of

[†] L. Eötvös University.
[‡] Brandeis University.

(1) Part 48 in the series Systematic Design of Chemical Oscillators. Part 47: Rábai, G.; Epstein, I. R. *Inorg. Chem.*, to be published.

(2) Epstein, I. R.; Orbán, M. In *Oscillations and Traveling Waves in Chemical Systems*; Field, R. J., Burger, M., Eds.; Wiley: New York, 1985; pp 257–286.

(3) Burger, M.; Field, R. J. *Nature (London)* **1984**, *307*, 720.

(4) Orbán, M.; Epstein, I. R. *J. Am. Chem. Soc.* **1985**, *107*, 2302.

(5) Orbán, M.; Epstein, I. R. *J. Am. Chem. Soc.* **1987**, *109*, 101.

(6) Orbán, M. *J. Am. Chem. Soc.* **1986**, *108*, 6893.

(7) Ouyang, Q.; De Kepper, P. *J. Phys. Chem.* **1987**, *91*, 6040.

0002-7863/89/1511-2891$01.50/0

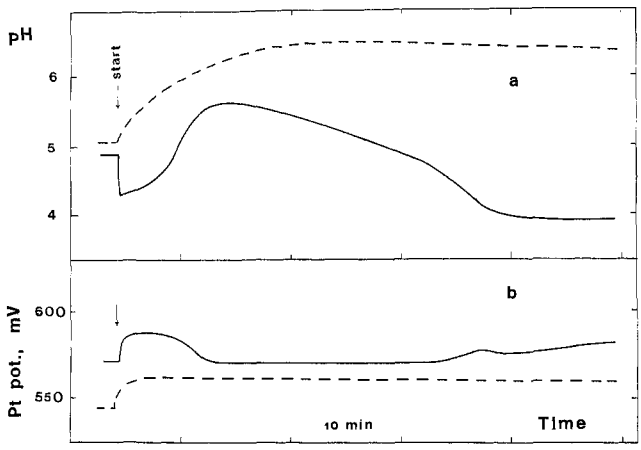

Figure 1. pH (a) and Pt electrode potential (b) vs time in the uncatalyzed $K_2S_2O_8$–$Na_2S_2O_3$ batch reaction. Initial concentrations: $[K_2S_2O_8]$ = 0.025 M, $[Na_2S_2O_3]$ = 0.0025 M (solid line), and 0.025 M (dashed line). Reaction was initiated by adding $K_2S_2O_8$ to the $Na_2S_2O_3$ solution.

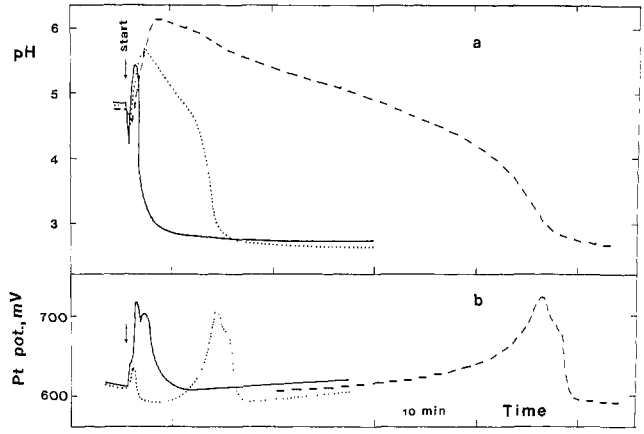

Figure 2. pH (a) and Pt electrode potential (b) vs time in the Cu^{2+}-catalyzed $K_2S_2O_8$–$Na_2S_2O_3$ batch reaction. Initial concentrations: $[K_2S_2O_8]$ = 0.025 M, $[CuSO_4]$ = 2.5 × 10^{-5} M, $[Na_2S_2O_3]$ = 0.0025 M (solid line), 0.01 M (dotted line), and 0.025 M (dashed line). Reaction was initiated by adding $K_2S_2O_8$ to the solution of $Na_2S_2O_3$ and $CuSO_4$.

mechanistic behavior than do their group VIIA counterparts.

We present here a new oscillatory system based on the chemistry of sulfur compounds. The reaction between $S_2O_8^{2-}$ and $S_2O_3^{2-}$ in the presence of trace amounts of cupric ion proceeds in an oscillatory fashion in a continuous flow stirred tank reactor (CSTR). In this report we describe the experimental observations and suggest a free-radical mechanism to account for the observed behavior.

The system investigated here suggests some interesting analogies with another non-halogen oscillator, the Jensen reaction,[8] i.e., the cobalt-catalyzed air oxidation of benzaldehyde. Mechanistic analysis of the oscillatory behavior in that reaction,[9,10] which is of considerable interest in synthetic organic chemistry, has yielded new insights into its workings. The peroxodisulfate–thiosulfate reaction is also of synthetic importance, serving as a source of free radicals to initiate the polymerization of vinyl monomers.[11,12] We hope that the present study and further mechanistic work growing out of it will give rise to a deeper understanding of this important reaction.

Experimental Section

Materials. All chemicals used were of analytical purity. The peroxodisulfate solutions were prepared from $K_2S_2O_8$. Some initial experiments were carried out with $(NH_4)_2S_2O_8$. However, the resulting solution is quite acidic owing to hydrolysis, and because of the pH dependence of the oscillations, we elected to use the potassium salt. Peroxodisulfate solutions slowly decompose during storage, so freshly prepared solutions were used in all experiments.

The $Na_2S_2O_3$ stock solutions can be stored for several weeks without appreciable decomposition. Their concentration was checked every 2 days by iodometric titration.

Cu(II) ions were introduced as $CuSO_4$ at levels $\leq 5 \times 10^{-5}$ M. To reduce the uncertainty in the low concentration of Cu^{2+}, a 10^{-3} M $CuSO_4$ stock solution acidified to pH 3 with H_2SO_4 to suppress the Cu^{2+} hydrolysis was used to make the appropriate dilution for each experiment.

Apparatus and Methods. The flow experiments were carried out at temperatures in the range 11.2–35.0 °C in a thermostated CSTR of volume 29.5 cm^3 fed with four input streams through a peristaltic pump. The Sage 375A pump allowed us to vary the flow rate, expressed as the reciprocal residence time k_0, from 0 to 1.5 × 10^{-2} s^{-1}. There was no air gap between the liquid surface and the reactor cap. The reactor was equipped with a bright Pt electrode, a $Hg_2SO_4|Hg|K_2SO_4$ reference electrode (Radiometer), and a combined glass electrode (Orion). A pH meter was used to record the pH simultaneously with the potential of the Pt electrode on a double channel recorder. The design of the reactor enabled us to introduce N_2 or O_2 gas into the reaction mixture. In some experiments the O_2 concentration in the overflow stream from the reactor was determined with a Clark-type oxygen electrode (Hansastech Ltd.). Some batch experiments were also performed in the O_2 measuring cell.

Results

Batch Experiments. We first studied the uncatalyzed reaction between neutral solutions of $K_2S_2O_8$ and $Na_2S_2O_3$. When the peroxodisulfate is in excess (Figure 1a, solid line), the pH rises slowly and then decreases even more slowly in a mildly sigmoidal fashion to its final value. When the initial concentrations of the reactants are equal (Figure 1a, dashed line), the curve is flatter, with the pH remaining near its maximum for nearly the entire course of the reaction. The potential of the Pt electrode varies little during the pH change (Figure 1b), while the O_2 electrode reveals a slow oxygen consumption (not shown) during the pH increase.

The presence of Cu(II), even at concentrations of 10^{-6}–10^{-5} M, markedly accelerates all the changes observed in the uncatalyzed system. The increase in pH, especially at low $[S_2O_3^{2-}]$, is nearly instantaneous. After reaching its maximum, the pH decreases at a rate inversely proportional to the initial thiosulfate concentration. The sigmoidal character of the curve is more pronounced, and the final pH is lower than in the uncatalyzed reaction (Figure 2a). Now the potential of the Pt electrode (Figure 2b) shows a definite increase followed by a decrease during the time of the sigmoidal pH drop. The shape of this peak resembles the oscillatory Pt response observed in the CSTR experiments described below. The oxygen electrode reveals a rapid consumption of the dissolved O_2. After a brief induction period, $[O_2]$ decreases almost to zero and then increases very slowly over the remaining course of the batch reaction.

Flow Experiments. The uncatalyzed reaction between $K_2S_2O_8$ and $Na_2S_2O_3$ in the CSTR yields a steady state under the entire range of conditions we have studied. The pH of this state varies somewhat with the input concentrations and flow rate but is generally above 5. This steady state pH suggests a relatively small conversion of reactants to products, so that the final composition closely resembles that of the input flow.

Introduction of a catalytic amount of Cu^{2+} with the input flow sharply increases the extent of reaction, much as Cu(II) enhances the batch reaction (cf. Figures 1 and 2). Depending upon the composition and flow rate of the input stream, we find either a low (2.5–3.5) pH steady state, sustained oscillation, or a high (>5) pH steady state. The location of these states in the input $[K_2S_2O_8]_0$–$[Na_2S_2O_3]_0$ plane is shown in Figure 3. Within a closed region of this phase diagram, we observe oscillations in the pH, in the potential of the Pt electrode and in the concentration of dissolved oxygen. Simultaneous recordings of these responses are presented in Figure 4. Periods, some of which are indicated in Figure 3, range from 5 to more than 60 min. At very high

(8) Jensen, J. H. *J. Am. Chem. Soc.* **1983**, *105*, 2639.
(9) Roelofs, M. G.; Wasserman, E.; Jensen, J. H. *J. Am. Chem. Soc.* **1987**, *109*, 4207.
(10) Noyes, R. M.; Yuan, Z., submitted for publication.
(11) Bacon, R. G. R. *Trans. Faraday Soc.* **1946**, *42*, 140.
(12) Morgan, L. B. *Trans. Faraday Soc.* **1946**, *42*, 169.

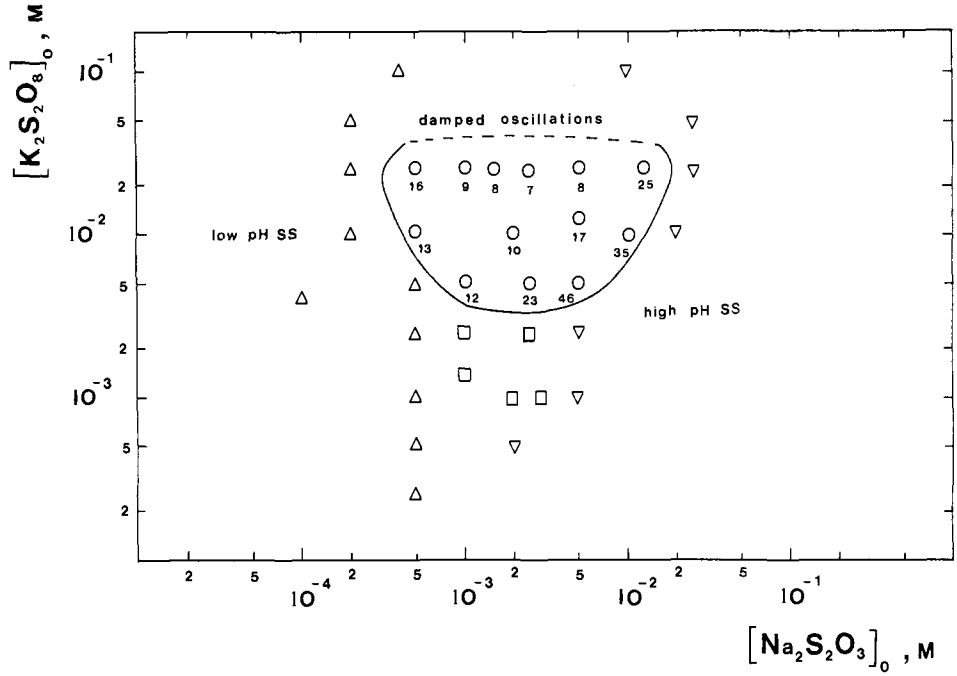

Figure 3. Phase diagram for the Cu^{2+}-catalyzed $K_2S_2O_8$–$Na_2S_2O_3$ reaction in the CSTR. Shown is the input $[K_2S_2O_8]_0$–$[Na_2S_2O_3]_0$ plane at fixed flow rate ($k_0 = 1.1 \times 10^{-3}$ s^{-1}) and temperature (25 °C). Symbols: ○, oscillations (numbers below the circles give oscillation periods in min); △, low pH steady state; ▽, high pH steady state; □, at these points the pH exhibits an intermediate value. If the flow rate is varied at these points with the other constraints held fixed, a sigmoidal pH vs flow curve is obtained.

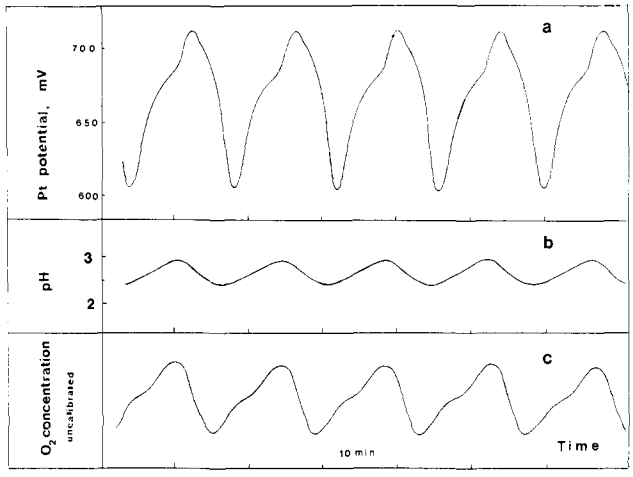

Figure 4. Oscillations in (a) potential of a Pt electrode, (b) pH, and (c) oxygen concentration in the Cu^{2+}-catalyzed $K_2S_2O_8$–$Na_2S_2O_3$ reaction: $[K_2S_2O_8]_0 = 0.025$ M, $[CuSO_4]_0 = 2.5 \times 10^{-5}$ M, $[Na_2S_2O_3]_0 = 0.005$ M, $k_0 = 3.5 \times 10^{-3}$ s^{-1}, $T = 25$ °C.

$[S_2O_8^{2-}]_0$, damped oscillations appear (dashed line) as the flow rate is decreased to the value in Figure 3.

The pH oscillations are rather modest in amplitude (0.05–0.6 units) and are always centered about pH ~3. They increase in amplitude as we move from left to right across the oscillatory domain in Figure 3. The amplitude of the oscillations in Pt potential is also less than in most other chemical oscillators, typically 40–50 mV and rarely exceeding 100 mV. These oscillations increase somewhat in both amplitude and complexity of waveform as the flow rate is increased. We note that the oscillations in Pt potential and pH found by Ouyang and De Kepper[7] in the silver-catalyzed sulfide–peroxodisulfate reaction are similar in amplitude to those reported here.

The O_2 oscillations resemble those of the Pt potential in shape, but are slightly shifted in phase, while they coincide perfectly in phase with the pH oscillations, higher pH corresponding to higher $[O_2]$. The oxygen concentration oscillates about a very low mean level, and the amplitude is only about 10–20% of the signal from an air-saturated solution.

Outside the oscillatory region, the system approaches either the low or the high pH steady state. We have not observed hysteresis between these states at the fixed flow rate of Figure 3. By varying the flow rate in either direction we can induce transitions between the steady states, but we have not found any evidence of bistability.

Effect of [Cu(II)]. As we have noted, cupric ions are essential for the oscillations. With $[S_2O_8^{2-}]_0 = 0.025$ M and $[S_2O_3^{2-}]_0 = 0.005$ M, introduction of an input flow of $[Cu^{2+}]_0 = 10^{-6}$ M noticeably accelerates the reaction, resulting in a steady state pH of ~3, but no oscillations appear. At 10^{-5} M Cu^{2+}, we find oscillations at higher flow rates ($k_0 = 4 \times 10^{-3}$ s^{-1}), but these are irregular with long period and slightly damped. They do, however, show large amplitude (>1 unit) variations in pH. With $[Cu^{2+}]_0 = 2.5 \times 10^{-5}$ M, we obtain regular oscillations in both Pt potential and pH (ΔpH = 0.3) for k_0 between 1×10^{-3} and 4×10^{-3} s^{-1}. When $[Cu^{2+}]_0$ is raised to 5×10^{-5} M, oscillation occurs only when k_0 is quite low ($< 1 \times 10^{-3}$ s^{-1}), and the amplitude of the pH oscillations is only about 0.05 units. A slight turbidity and yellowish color appear and vanish periodically. We conclude that the optimal Cu^{2+} input concentration for oscillations is in the range $1–5 \times 10^{-5}$ M.

Effects of Other Metal Ions. We tested several other metal ions—Ag^+, Fe^{2+}, Fe^{3+}, Mn^{2+}, VO^{2+}, Hg^{2+}, and Os(VIII)—to ascertain whether they could induce oscillatory behavior in the $K_2S_2O_8$–$Na_2S_2O_3$ reaction. With the exception of Fe^{3+}, none was at all effective in catalyzing the peroxodisulfate–thiosulfate reaction. Ferric ion oxidizes $S_2O_3^{2-}$, and the Fe^{2+} formed is rapidly oxidized back to Fe^{3+} by $S_2O_8^{2-}$. However, the catalytic effect of ferric ions appears to be too small to generate oscillations, most likely because of the hydrolysis of Fe^{3+} in the nearly neutral solution. Acidifying the solution to suppress the hydrolysis is likely to promote the decomposition of the thiosulfate.

It is surprising that Ag^+, the best known catalyst in $S_2O_8^{2-}$ oxidations, is ineffective in the present system. Silver ions have been reported to catalyze the oscillatory $S_2O_8^{2-}$–S^{2-} and $S_2O_8^{2-}$–$H_2C_2O_4$ reactions[7,13] in acidic solution but had no effect on the $S_2O_8^{2-}$–$S_2O_3^{2-}$ system. Although we have not proved that Cu^{2+} is the only metal ion with a significant effect on this reaction,

(13) Ouyang, Q.; De Kepper, P., submitted for publication.

our results strongly suggest both that its presence is essential for and that it is the most effective catalyst of oscillatory behavior in the peroxodisulfate–thiosulfate reaction.

Effects of Acid, Base, and Buffer. Most of our experiments were carried out with neutral solutions of $S_2O_8^{2-}$ and $S_2O_3^{2-}$. Because the pH oscillates, we decided to test the effects of adding acid, base, and buffer solutions to the input composition of Figure 4. Introduction of $[NaOH]_0 = 10^{-3}$ M gives oscillations with slightly lower amplitude in the Pt electrode potential and higher amplitude ($\Delta pH = 0.5$) in the pH. When the input of base is increased to 5×10^{-3} M, the oscillations cease, though the final pH remains low, at 2.8. With $[H_2SO_4]_0 = 10^{-3}$ M, we get a slightly enhanced Pt signal but smaller ($\Delta pH = 0.15$) pH oscillations, while $[H_2SO_4]_0 = 5 \times 10^{-3}$ M suppresses the oscillations completely. No oscillations are obtained in pH 4 K-biphthalate buffer. Introducing pH 3 K-biphthalate–HCl buffers stops the pH oscillations immediately, while the Pt oscillations gradually damp and cease only after 7–8 further cycles.

We conclude that the oscillatory dynamics function best in the absence of added acid, base, or buffer. The system, as a result of competing H^+- and OH^--producing processes, generates internally sufficient acid to adjust the pH to the value about which it oscillates. Any interference with the delicate balance makes oscillation less likely.

Effects of O_2 and N_2. From Figure 4c, it appears that O_2 is an intermediate in the oscillatory process. Oxygen has been reported to be an inhibitor in at least one Ag^+-catalyzed peroxodisulfate oxidation.[14]

We have investigated the effects of bubbling O_2 and N_2 through the reaction mixture in the reactor and/or through the input solutions. Somewhat surprisingly we find no inhibitory effect of O_2 but rather the opposite. In many cases, oxygen bubbling increases the amplitude of both the Pt and pH oscillations and can even induce oscillations under conditions that would yield steady-state behavior in the absence of added O_2. This last effect is seen primarily in the high pH steady state, i.e., oxygen causes the oscillatory domain in Figure 3 to shift to the right. Nitrogen bubbling tends to decrease the amplitudes of oscillation and in some cases causes the cessation of oscillation.

Given the lack of an air gap above the reactor solution, it appears that the O_2 generated by the reaction is an important component in the oscillation. After making these observations, we took no further precautions to remove dissolved oxygen from our stock and input solutions.

Temperature Effects. Experiments on other oscillatory systems show that temperature may have a significant effect on the dynamical behavior. Oscillations may occur only within a narrow temperature range,[15] or a regular oscillatory pattern may become chaotic on changing the temperature.[16]

Experiments were carried out with the oscillatory composition of Figure 4 at four different temperatures: 12, 18, 25, and 35 °C. Periodic oscillations occurred at all temperatures with slightly increasing amplitude and decreasing period (24, 14, 8, and 4.5 min, respectively) as the temperature was raised. Thus the dynamical behavior in the present system is relatively insensitive to temperature.

Discussion

The peroxodisulfate–thiosulfate reaction has been the subject of several studies because of its importance as a source of free radicals to initiate vinyl polymerization.[11,12] The uncatalyzed reaction is very slow, but trace amounts of Cu^{2+} markedly increase the rate. The stoichiometry with or without the copper catalyst is[17]

$$S_2O_8^{2-} + 2S_2O_3^{2-} \rightarrow 2SO_4^{2-} + S_4O_6^{2-} \quad (1)$$

The rates of both the uncatalyzed and the catalyzed reactions are independent of the thiosulfate concentration and first order in $[S_2O_8^{2-}]$. For the reaction in the presence of Cu^{2+}, the rate law is[18]

$$-d[S_2O_3^{2-}]/dt = k[S_2O_8^{2-}][Cu^{2+}] \quad (2)$$

with $k = 16.6\ M^{-1}\ s^{-1}$. A radical chain mechanism has been proposed for the uncatalyzed reaction,[19] but no suggestion has yet been offered to account for the catalyzed pathway.

We consider first the likely intermediates formed when peroxodisulfate and thiosulfate interact in the presence of catalytic amounts of Cu(II). The $S_2O_8^{2-}$ ion is a very strong oxidant ($S_2O_8^{2-} + 2e^- = 2SO_4^{2-}$, $E^0 = 2.01$ V). However, peroxodisulfate oxidations are generally slow. It has been suggested[20] that $S_2O_8^{2-}$ may be converted to sulfate via two different routes of electron uptake: (a) by a symmetrical fission of $S_2O_8^{2-}$ to two $SO_4^{\bullet-}$ radical anions, which are then reduced to SO_4^{2-} ($S_2O_8^{2-} + e^- = SO_4^{\bullet-} + SO_4^{2-}$, $E^0 = 1.6$ V[14b]) or may be oxidized to the neutral intermediate species SO_4 if a sufficiently strong oxidant is present; (b) by an asymmetrical decomposition to SO_4^{2-} and SO_4, with the latter then serving to oxidize the reductant. Kolthoff and Miller[20] suggest $SO_4^{\bullet-}$ and SO_4 as the key intermediates, respectively, in the uncatalyzed and H^+-catalyzed decompositions of $S_2O_8^{2-}$ in aqueous solution.

Thiosulfate ion is a strong reductant and can form both $S_2O_3^{\bullet-}$ radicals and neutral S_2O_3 as intermediates. It can give rise to $S_4O_6^{2-}$ through the combination either of two $S_2O_3^{\bullet-}$ radicals or of one S_2O_3 and one $S_2O_3^{2-}$.

The most common oxidation state of copper is Cu^{2+}. However, strong reductants can easily reduce it to Cu^+ ($Cu^{2+} + e^- = Cu^+$, $E^0 = 0.3$ V), while strong oxidants may oxidize it to Cu^{3+} ($Cu^{3+} + e^- = Cu^{2+}$, $E^0 \approx 1.6$–1.8 V). In fact, standard solutions of Cu(III) are prepared[21] by reacting $CuSO_4$ with $K_2S_2O_8$. Earlier studies of the catalytic effect of Cu(II) on peroxodisulfate oxidations have invoked both Cu^+ [12,17,18] and Cu^{3+} [14,22,23] to explain the cyclic oxidation–reduction processes.

With the above features of the underlying chemistry in mind, we can give a qualitative description of the batch and flow behaviors of the $S_2O_8^{2-}$–$S_2O_3^{2-}$–Cu^{2+} system. Figures 1a and 2a portray a pH change that is not predicted by the overall stoichiometry of reaction 1. Sorum and Edwards[19] suggest that the observed pH changes result from side reactions, and our experiments support their proposal. The oxygen consumption found to accompany the pH change implies that the rise in pH during the early part of the reaction results from the uptake of dissolved O_2 by the reducing free radical $S_2O_3^{\bullet-}$ formed either in the initial part of the slow uncatalyzed $S_2O_8^{2-}$–$S_2O_3^{2-}$ reaction (Figure 1a) or, in the case of the catalyzed system, in the fast reaction between cupric and thiosulfate ions. We also note that bubbling O_2 through the solution resulted in a higher maximum pH in the oscillatory state. These processes may be described by eq 3–5 and 7 or 6 and 7 for the uncatalyzed and catalyzed reactions, respectively.[24]

$$S_2O_8^{2-} \rightarrow 2SO_4^{\bullet-} \quad (3)$$

$$SO_4^{\bullet-} + H_2O \rightarrow HSO_4^- + OH^\bullet \quad (4)$$

$$OH^\bullet + S_2O_3^{2-} \rightarrow OH^- + S_2O_3^{\bullet-} \quad (5)$$

$$Cu^{2+} + S_2O_3^{2-} \rightarrow Cu^+ + S_2O_3^{\bullet-} \quad (6)$$

$$O_2 + 4H^+ + 4S_2O_3^{2-} \rightarrow 2H_2O + 2S_4O_6^{2-} \quad (7)$$

(14) (a) Allen, T. L. *J. Am. Chem. Soc.* **1951**, *73*, 3589. (b) Wilmarth, W. K.; Haim, A. In *Peroxide Reaction Mechanisms*; Edwards, J. O., Ed.; Wiley: New York, 1961; p 175.
(15) Kumpinsky, E.; Epstein, I. R. *J. Phys. Chem.* **1985**, *89*, 688.
(16) Orbán, M.; Epstein, I. R. *J. Phys. Chem.* **1982**, *86*, 3907.
(17) King, C. V.; Steinbach, O. I. *J. Am. Chem. Soc.* **1930**, *52*, 4479.
(18) Patat, F.; Prölss, H. *Ber. Bunsenges. Phys. Chem.* **1967**, *71*, 1095.
(19) Sorum, C. H.; Edwards, J. O. *J. Am. Chem. Soc.* **1952**, *74*, 1204.
(20) Kolthoff, I. M.; Miller, I. K. *J. Am. Chem. Soc.* **1951**, *73*, 3055.
(21) Berka, A. *Newer Redox Titrants*; Pergamon: Oxford, 1965; pp 14–15.
(22) Ball, D. L.; Crutchfield, M. M.; Edwards, J. O. *J. Org. Chem.* **1960**, *25*, 1599.
(23) Bhakuni, R. S.; Srivastava, S. P. *Z. Phys. Chem.* **1960**, *213*, 129.
(24) Heckel et al. (Heckel, E.; Henglein, A.; Beck, G. *Ber. Bunsenges. Phys. Chem.* **1966**, *70*, 149) found by pulse radiolysis that the reverse of reaction 4 has a rate constant of $8 \times 10^5\ M^{-1}\ s^{-1}$, but under our experimental conditions, this process is unlikely to play a major role.

where eq 7 represents the overall stoichiometry of several elementary steps with rate law[19]

$$-d[H^+]/dt = k[S_2O_3^{\bullet-}][O_2][H^+]$$

The origin of the pH decreases after the maximum is more difficult to interpret. Oxidation of a small portion of the thiosulfate beyond tetrathionate (e.g., to sulfite) or Cu^{2+}-catalyzed decomposition of peroxodisulfate to sulfuric acid via $SO_4^{\bullet-}$ are likely sources for the H^+ generated.

Although the batch behavior can be understood, at least qualitatively, in terms of reactions 3–7 and accompanying side reactions, it is clear that a mechanistic explanation of the oscillatory behavior must go beyond eq 3–7. We must seek other reactions that can generate the necessary positive and negative feedback and can account for both the pH and O_2 oscillations. The observed low amplitude of the pH oscillations suggests that the present system differs mechanistically from such high pH amplitude oscillators as hydrogen peroxide–sulfide[4] and hydrogen peroxide–thiosulfate–Cu(II).[5] In those systems, the periodic variation in pH appears to represent the *driving force* for the oscillatory behavior, while here it seems to be rather a *consequence* of oscillations generated through other aspects of the chemistry.

The catalytic cycle in the $S_2O_8^{2-}$–$S_2O_3^{2-}$–Cu^{2+} system may be represented schematically as The diagram shows how the oxi-

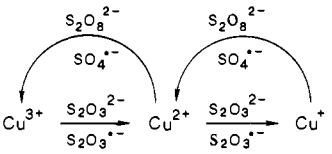

dation state of copper changes as the system cycles through the various processes, in which the sulfur reactants are shown above the arrows and the intermediates below.

A more detailed version of this scheme is contained in the elementary step mechanism, eq M1–M15, of Scheme I. Reactions

Scheme I. Elementary Steps in the Cu^{2+}-Catalyzed $S_2O_8^{2-}$–$S_2O_3^{2-}$ Reaction

$$S_2O_3^{2-} + Cu^{2+} \rightarrow Cu^+ + S_2O_3^{\bullet-} \quad (M1)$$

$$S_2O_3^{\bullet-} + S_2O_8^{2-} \rightarrow SO_4^{2-} + SO_4^{\bullet-} + S_2O_3 \quad (M2)$$

$$S_2O_3 + S_2O_3^{2-} \rightarrow 2S_2O_3^{\bullet-} \quad (M3)$$

$$2S_2O_3^{\bullet-} \rightarrow S_4O_6^{2-} \quad (M4)$$

$$Cu^+ + S_2O_8^{2-} \rightarrow Cu^{2+} + SO_4^{2-} + SO_4^{\bullet-} \quad (M5)$$

$$Cu^{2+} + S_2O_8^{2-} \rightarrow Cu^{3+} + SO_4^{2-} + SO_4^{\bullet-} \quad (M6)$$

$$Cu^{3+} + SO_4^{\bullet-} \rightarrow Cu^{2+} + SO_4 \quad (M7)$$

$$Cu^{3+} + S_2O_3^{2-} \rightarrow Cu^{2+} + S_2O_3^{\bullet-} \quad (M7')$$

$$SO_4 + SO_4^{2-} \rightarrow 2SO_4^{\bullet-} \quad (M8)$$

$$S_2O_3^{\bullet-} + SO_4^{2-} \rightarrow SO_4^{\bullet-} + S_2O_3^{2-} \quad (M8')$$

$$2SO_4^{\bullet-} \rightleftarrows S_2O_8^{2-} \quad (M9)$$

$$SO_4^{\bullet-} + H_2O \rightarrow HSO_4^- + OH^\bullet \quad (M10)$$

$$S_2O_3^{2-} + OH^\bullet \rightarrow S_2O_3^{\bullet-} + OH^- \quad (M11)$$

$$HSO_4^- \rightleftarrows H^+ + SO_4^{2-} \quad (M12)$$

$$S_2O_3^{\bullet-} + O_2 + H^+ \rightarrow HO_2^\bullet + S_2O_3 \quad (M13)$$

$$2HO_2^\bullet \rightarrow H_2O_2 + O_2 \quad (M14)$$

$$H_2O_2 + OH^\bullet \rightarrow HO_2^\bullet + H_2O \quad (M15)$$

(M1–M9) constitute the essential steps in the oscillatory process. By adding steps M1–M8 plus 2 × M9, we obtain the overall stoichiometry of eq 1. By taking step M6 to be rate determining, we obtain the correct rate law, eq 2, for the Cu^{2+}-catalyzed reaction.

Two autocatalytic loops can be generated from the core mechanism, steps M1–M9. The sequence M1 + M2 + M3 gives

$$Cu^{2+} + 2S_2O_3^{2-} + S_2O_8^{2-} + S_2O_3^{\bullet-} \rightarrow Cu^+ + SO_4^{2-} + SO_4^{\bullet-} + 3S_2O_3^{\bullet-}$$

for which M2 is almost surely rate determining, since the other two reactions are simple electron transfers. Adding M5, we may write this loop as

$$Cu^{2+} + 2S_2O_3^{2-} + 2S_2O_8^{2-} + S_2O_3^{\bullet-} \rightarrow Cu^{2+} + 2SO_4^{2-} + 2SO_4^{\bullet-} + 3S_2O_3^{\bullet-}$$

The second autocatalytic sequence consists of M7 + M8

$$Cu^{3+} + SO_4^{2-} + SO_4^{\bullet-} \rightarrow Cu^{2+} + 2SO_4^{\bullet-}$$

or adding M6

$$Cu^{2+} + S_2O_8^{2-} + SO_4^{\bullet-} \rightarrow Cu^{2+} + 3SO_4^{\bullet-}$$

The first loop is composed of fast reactions; M1 is taken to be nearly instantaneous, generating an initial $S_2O_3^{\bullet-}$ radical concentration comparable to that of the input $[Cu^{2+}]_0$. Therefore, the slower second loop will be the more important contributor to the positive feedback in the system. The role of the negative feedback is played by the chain termination steps M4 and M9. Although sulfate ion, which is formed in several steps, is consumed in step M8, it is unlikely that $[SO_4^{2-}]$ shows significant oscillations. The oscillations in Pt potential are primarily attributable to redox couples involving copper species.

An alternative version of the second autocatalytic loop may be constructed by utilizing steps M7′ and M8′ in place of M7 and M8 in Scheme I. Now the autocatalysis involves the $S_2O_3^{\bullet-}$ radical just as in the first loop instead of SO_4, but the second loop comes into play only after the oxidation of copper to Cu(III) is complete and the reagent $S_2O_3^{2-}$ has been replenished by the flow. The two loops are separated by the rate-determining reaction M6. The autocatalytic process now consists of M7′ + M8′ + M3:

$$Cu^{3+} + 2S_2O_3^{2-} + SO_4^{\bullet-} + S_2O_3^{\bullet-} \rightarrow Cu^{2+} + SO_4^{2-} + 3S_2O_3^{\bullet-}$$

Adding M6, we obtain the composite Cu^{2+}-catalyzed autocatalytic reaction of peroxodisulfate and thiosulfate ions:

$$Cu^{2+} + 2S_2O_3^{2-} + S_2O_8^{2-} + S_2O_3^{\bullet-} \rightarrow Cu^{2+} + 2SO_4^{2-} + 3S_2O_3^{\bullet-}$$

Further addition of M4 yields the overall stoichiometry of eq 1.

From the small magnitude of the pH and O_2 oscillations that accompany the more pronounced variations in the Pt potential, we conclude that the pH and $[O_2]$ changes arise from secondary steps, such as M10–M15. The pH decreases in M10 and M12 and may increase as a result of M11 or eq 7. Oxygen is formed in steps M14 and consumed in M13 or in eq 7.

Even the above mechanistic picture of the $S_2O_8^{2-}$–$S_2O_3^{2-}$–Cu^{2+} oscillator is less than complete. The copper ions are almost certainly complexed in each oxidation state, for example as $[Cu^I(S_2O_3)_2]^{3-}$ and $[Cu^I(S_2O_3)]^{-}$[18] or as $[Cu^I(S_2O_8)]^-$.[25] Further steps involving plausible fates of the various radical species undoubtedly come into play.[26] The effects of added acid, base, and buffer on the oscillations remain unaccounted for.[27] Nevertheless, the core mechanism proposed here together with a limited number

(25) Reference 30 in the following: House, D. A. *Chem. Rev.* **1962**, *62*, 185.

(26) Hayon, E.; Treinin, A.; Wilf, J. *J. Am. Chem. Soc.* **1972**, *94*, 47.

(27) Steps involving the protonation of various sulfur-containing intermediates and/or taking into account the influence of H^+ on the relative amounts of symmetric and asymmetric decomposition of $S_2O_8^{2-}$ should help here.

of additional side reactions should serve as a solid starting point for detailed numerical simulations of this system to be undertaken in our laboratories.

Acknowledgment. We thank Yin Luo, Kenneth Kustin, and Patrick De Kepper for thoughtful discussions. This work was supported by the National Science Foundation (CHE-8800169) and by a U.S.-Hungarian Cooperative Grant from the NSF (INT-8613532) and the Hungarian Academy of Sciences. The oxygen electrode was purchased through a grant from the Gillette Company.

Registry No. $S_2O_8^{2-}$, 15092-81-6; $S_2O_3^{2-}$, 14383-50-7; Cu, 7440-50-8; O_2, 7782-44-7.

Carbon-Hydrogen Bond Activation in Novel η^2-Bound Cationic Heterocycle Complexes of Pentaammineosmium(II)

Rossella Cordone, W. Dean Harman, and Henry Taube*

Contribution from the Chemistry Department, Stanford University, Stanford, California 94305.
Received September 21, 1988

Abstract: Reduction of $(NH_3)_5Os(TFMS)_3$ (TFMS = trifluoromethanesulfonate) by $Co(Cp)_2$ in the presence of cationic pyridines L (L = *N*-methylpyridinium, lutidinium, pyridinium, and *N*-methyl-4-picolinium) leads to the formation of isolable pentaammineosmium(II) π complexes featuring fluxional 3,4-η^2 ligands for the former three and 2,3-η^2 for the latter. Analogously to the previously reported η^2-lutidine analogue, activation at the C4-H bond was observed for the 3,4-η^2-bound cationic ligands, yielding σ carbon-bound pyridinium ylides. In accord with observations made on other complexes containing metal-ylide carbon bonds, the resulting pentaammineosmium(II) *N*-methylpyridinium complex is unstable with respect to loss of the trans ammine.

Numerous reports on the subject of arene carbon-hydrogen bond activation by transition-metal centers exist.[1] The enhanced reactivity generally observed for arenes as compared to alkanes has been attributed to the ability of the former to form η^2-bound intermediates,[2] a pathway not available for saturated hydrocarbons. However, evidence for the existence of such complexes until recently was only indirect, as their instability rendered their identification difficult.

A recently reported example of an isolable η^2-bound precursor for aromatic C-H activation came with the discovery of the complex $[(NH_3)_5Os(\eta^2\text{-}2,6\text{-lutidine})]^{2+}$ in our laboratories.[3] This η^2 species is stable for hours in a variety of solvents; however, it undergoes intramolecular rearrangement with time to yield a carbon-bound lutidinium ylide, where the osmium moiety resides at C4 of the aromatic ring.

The observations on this complex motivated us to extend the chemistry of pentaammineosmium(II) to include cationic nitrogen heterocycles, which relative to the neutral heterocycle are better π acceptors but extremely weak nucleophiles. We report here the preparation and characterization of a series of stable complexes containing η^2-bound pyridinium ligands, the majority of which, in analogy to the previously reported lutidine complex, also proved to be precursors to activation of the aromatic C4-H bond.

Experimental Section

Abbreviations: DMA = *N*,*N*-dimethylacetamide; DME = 1,2-dimethoxyethane; TFMS = trifluoromethanesulfonate; NMepy = *N*-methylpyridinium; Hlu = 2,6-lutidinium (2,6-dimethylpyridinium); Hpy = pyridinium; NMepic = *N*-methyl-4-picolinium (1,4-dimethylpyridinium).

Instrumentation and Techniques. All nonaqueous reactions were carried out in a Vacuum Atmospheres Corp. glovebox under an argon atmosphere. All solvents were fully deoxygenated by purging with argon for 45 min. ^1H NMR spectra were recorded on a Varian XL-400 spectrometer. Cyclic voltammograms were recorded on a Princeton Applied Research Model 173 potentiostat and Model 175 universal programmer. A platinum button was used as a working electrode. A platinum wire was the auxiliary electrode, and a gold button immersed in 0.5 M NaTFMS in DME acted as the reference electrode; this electrode was separated from the bulk solution by a Vycor tip. The $Fe(Cp)_2^+/Fe(Cp)_2^0$ couple was used as a reference in situ. Voltammograms were recorded on a Hewlett-Packard 7045A X-Y recorder. The voltage range was -1.20 to +1.20 V vs NHE, and the scan rate was typically 200 mV/s. Electrochemical analysis of bulk solutions was performed by the use of a modified rotating disk technique described by Harman.[4]

Purifications and Preparations. Solvents. 1,2-Dimethoxyethane and diethyl ether were refluxed for 5 h over NaK alloy and distilled under argon. Methylene chloride was refluxed for 8 h over P_2O_5 and distilled under argon. Acetone was stirred over B_2O_3 for 3 days at room temperature and vacuum distilled.[5] *N*,*N*-Dimethylacetamide was predried over BaO for 48 h, distilled from triphenylsilyl chloride, and redistilled from CaH_2 under vacuum. Ethyl acetate was stirred over CaH_2 for 8 h and distilled under argon. All solvents were thoroughly deoxygenated by purging with argon for 45 min.

Reagents. Magnesium turnings were activated by treating with iodine in DME under argon, stirring for several hours, and washing with DMA, DME, and ether. Pyridine, 4-picoline, and 2,6-lutidine were stirred over CaH_2 for 8 h and distilled under vacuum. In order to remove unhindered pyridine contaminants, predried 2,6-lutidine was treated following the method outlined by Shepherd et al.[6] Cobaltocene (Alfa), HTFMS, and CH_3TFMS (Aldrich) were used without further purification. $(NH_3)_5Os(TFMS)_3$ was prepared according to previously reported methods.[7]

Ligands. The following preparations were performed in a glovebox. *N*-Methylpyridinium, *N*-methylpicolinium, lutidinium, and pyridinium triflates were prepared by treating 1 mL of the corresponding bases dissolved in 4 mL of ethyl acetate with 1.5 mL of cold CH_3TFMS or HTFMS (caution!), respectively. Solids were obtained upon cooling these solutions to -40 °C for 30 min.

Osmium Compounds. $[(NH_3)_5Os(\eta^2\text{-NMepy})](TFMS)_3$ (**1**) was obtained by dissolving 75 mg of $(NH_3)_5Os(TFMS)_3$ and 0.5 of NMepyTFMS in ~5 mL of neat DME. A solution containing 19.6 mg of cobaltocene (1 equiv) dissolved in 1 mL of DME was added dropwise, with constant stirring. A black solid is present once the addition of cobaltocene is complete. This solid was stirred for 1 h in ~8 mL of DME and dried with ether. Anal. Calcd for $[(NH_3)_5Os(C_6H_8N)]$-

(1) E. G.: (a) Jones, W. D.; Feher, F. J. *J. Am. Chem. Soc.* **1984**, *106*, 1650. (b) Sweet, J. R.; Graham, W. A. G. *J. Am. Chem. Soc.* **1983**, *105*, 305.
(2) Parshall, G. W. *Homogeneous Catalysis*; Wiley-Interscience: New York, 1980; Chapter 7.
(3) Cordone, R.; Taube, H. *J. Am. Chem. Soc.* **1987**, *109*, 8101.
(4) Harman, W. D. Ph.D. Dissertation, Stanford University, 1987.
(5) Burfield, D. R.; Smithers, R. H. *J. Org. Chem.* **1978**, *43*, 3966.
(6) Shepherd, R. E.; Taube, H. *Inorg. Chem.* **1973**, *12*, 1392.
(7) Lay, P.; Magnuson, R.; Sen, J.; Taube, H. *J. Am. Chem. Soc.* **1982**, *104*, 7658.

0002-7863/89/1511-2896$01.50/0